Nanochem Res 8(1): 78-86 Winter 2023

RESEARCH PAPER

Comparative Studies of Chitosan-Silver Nanocomposites from Commercial and Biowaste Sources

Vincent Nwalieji Okafor *, Bankole Akinyele Abimbola, Assumpta Daberechukwu Iwe, Oluchukwu Francisca Mbume

Department of Pure and Industrial Chemistry, Nnamdi Azikiwe University, PMB 5025, Awka, Anambra State, Nigeria

ARTICLE INFO

Article History:
Received 20 Nov 2022
Accepted 27 Dec 2022
Published 31 Jan 2023

Keywords:
Chitosan
Biowaste
Nanoparticles
Silver
Spectroscopy

ABSTRACT

In this work, silver nanoparticles/chitosan nanocomposites were prepared for possible industrial and biomedical applications. Chemical reduction of silver nitrate salt produced silver nanoparticles (AgNPs). Low molecular weight chitosan (LMWCS) which connotes artificial chitosan (ArCS) was obtained, and biodegradable chitosan was extracted from snail shells using standard procedures. Sodium tripolyphosphate (TPP) was used to produce chitosan nanoparticles (snail shell nanochitosan (ScCSNPs) and artificial nanochitosan (ArCSNPs)) from extracted chitosan and LMWCS. AgNPs-CSNPs were produced by incorporating AgNPs into CSNPs as antimicrobial agents. Characterization of the chitosan doped silver nanoparticles was conducted using scanning electron microscopy (SEM), Fourier Transform Infrared Spectroscopy (FTIR), Differential Scanning Calorimetry (DSC) and X-ray Diffraction (XRD). The morphological properties of nanochitosan (ScCSNPs and ArCSNPs) and AgNPs-nanochitosan (ScCSNPs-AgNPs and ArCSNPs-AgNPs) indicated porosity and agglomeration, while functional groups -OH, -NH, and C-H were revealed. The presence of AgNPs in the polymeric matrix of nanochitosan was confirmed by a shift in some of the adsorption bands.

XRD and DSC results revealed that the nanochitosan is crystalline, and they also confirmed the presence of AgNPs in the chitosan polymeric matrix. The study established that chitosan extracted from snail shells, which contribute to environmental pollution, could be a good source for the preparation of nanocomposite materials, which are useful in a variety of industrial and biomedical applications.

How to cite this article
Okafor V. N., Abimbola B. A., Iwe A. D., Mbume O. F, Comparative Studies of Chitosan-Silver Nanocomposites from Commercial and Biowaste Sources. Nanochem Res, 2023; 8(1): 78-86 DOI: 10.22036/ncr.2023.01.008

INTRODUCTION

Chitosan and its derivatives hold immense promise in many industrial formulations due to their attractive properties such as compatibility, bio-adhesive, high drug loading, and high antimicrobial spectrum. Another advantage is that they can be sourced from shells, crabs, and shrimps which abound in Nigeria. The provision of raw materials for various industries is a highly important area of chemical research since Nigeria currently contends with heavy import burdens of such materials. With significant economic value, the shellfish industry is important in the fisheries sector but generates a massive amount of shell, a biowaste, that is unfriendly because it creates an unsanitary environment with a strong odor. This shell, as well as insects and fungus, contain protein, chitin, and minerals which are valuable resources that can be harnessed. Chitosan, a

* Corresponding Author Email: *vnw.okafor@unizik.edu.ng*

deacetylated chitin and a polysaccharide with numerous uses, can further be extracted from the shell waste [1-3]. The steps of extraction basically involve pretreatment of shell followed by deproteination and demineralization. The final step is deacetylation of the chitin to get chitosan [4, 5]. Chitosan, α (1, 4)-amino-2-deoxyβ-D glucan contains a number of beneficial properties that have piqued the curiosity of scientists over the last two decades [4]. Many researchers have studied chitosan and their derivatives because of their diverse applications in agriculture, engineering, biomedical, and pollution remediation due to their non-toxic, biocompatible, edible and adsorptive properties [2-6]. In pharmacology, chitosan has been applied for controlled drug release and wound healing owing to their hydrogel properties [5]. In addition, it is recently used for disinfection due to its antimicrobial properties [3, 6]. The various features of chitosan have drawn researchers' attention in recent years, generating significant interest in the field of biomedical engineering [7]. Based on these outstanding properties, chitosan nanoparticles (CSNPs) have defiled the questioned effect that nanosized materials have on nature and human systems. In fact, the well-known polymeric and cationic properties of chitosan nanoparticles (CSNPs) have sparked interest in their application [2]. One of the biopolymers used in the formation of metallic nanoparticles as a reducing agent and a protective polymer is chitosan. CSNPs is believed to be a higly promising candidate for use as a biomaterial in food-related applications. Because of their small size and high surface-to-weight ratio, CSNPs have been extensively studied in the biomedical field [3-7].

As versatile as CSNPs are, using high concentrations of their suspensions or quantity in industrial applications may not be cost-effective [8-9]. To reduce the effective concentration of CSNPs, a synergy of CSNPs with other materials for various applications has been initiated. For example, CSNPs and the antimicrobial alkaloid berberine have a synergic effect against B. Subtilis and S. aureus [8]. The traditional method of using TPP as an ionic cross-linker was replaced with cinnamaldehyde, which resulted in synergistic antibacterial activity [9]. Maximum E. coli inhibition of 85% was achieved with only 5% (v/v) doping of chitosan nanoparticles into the cellulose films [10]. Some metals and metal oxides that have beneficial properties were also considered in this synergistic exploitation of CSNPs. A few of these are Ag, ZnO, TiO_2, MgO and CuO. They possess strong antibacterial activity against a variety of bacterial pathogens [11].

Snail is a great source of protein which is used in most delicacies especially in southern part of Nigeria. However, the snail shells are not known to serve any useful purpose and form a component of waste materials from kitchens. The utilization of the shells in chitosan production is a very promising waste to wealth research. The extraction of snail shells into high-quality chitosan and subsequent doping with AgNPs becomes essential. Attempts have been made previously to convert waste materials to chitosan [11-17]. Nonetheless, no research of this kind has attempted a comparison of CSNPs synthesized from snail shell waste to CSNPs from LMWC, as well as a comparison of AgNPs-CSNPs synthesized from snail shell waste to AgNPs-CSNPs from LMWC. Therefore, the study and characterization of CSNPs derived from LMWC and CSNPs from snail shell and their composites with AgNPs would be of great interest. Hence, the aim of the current work is to examine the structural differences in the surface morphology, the FTIR bands, and changes in crystal structure and cell parameters of the CSNPs and the AgNPs-CSNPs produced.

EXPERIMENTAL

Materials

Snail shells were obtained from Eke-Awka market, Anambra State, Nigeria washed and dried under the sun for 6 hours before oven drying. Low molecular weight Chitosan (LMWC) was provided from Central Drug House (CDH) New Delhi, India. Other chemicals such as sodium tripolyphosphate (TPP), Sodium Hydroxide, sodium borohydride, silver nitrate, hydrochloric acid, acetic acid and potassium hydroxide used were analytically graded.

Preparation of Chitin and Chitosan

Chitosan was prepared based on the method described by Okoya *et al.* [18]. The snail shells were ground into powder and sieved through a 2 mm sieve. The sieved powdered snail shells were deproteinized by weighing 50 g of the shell powder into a 500 mL beaker and 200 mL of 4 % (w/v) KOH was added with constant stirring for 6 hr at 80 °C and then filtered. The residue was washed with distilled water until it was free of base, then dried for 2 hr at 100 °C. The deproteinized snail shell residue was

then placed in a 250 mL conical flask with 100 mL of 3 % (v/v) 1 M HCl and demineralized for 3 hr at 30°C on a magnetic stirrer. The content was filtered, and the residue was washed until it was acid-free. The acid-free residue was then dried for 1 hr at 90 °C. As a result, chitin, a snow-white residue, was obtained. For deacetylation, the chitin was poured into a 250 mL conical flask. A 50 percent (w/v) NaOH solution was added, stirred for 4 hr at 30°C, and filtered. After filtration, the chitosan residue was washed until the filtrate was neutral. It was then dried at 90°C for 1 hr and stored for further use.

Preparation of CSNPs from LMWC

Chitosan (2 g) was dissolved in 50 mL of 1% acetic acid with constant stirring. The pH of the resulting solution was maintained at 4 by using 1M HCl. A 100 mg of sodium tripolyphosphate was dissolved in 100 mL of 1M NaOH. This solution was added to the mixture of the acidified chitosan in drops with the aid of syringe until complete formation of precipitates. The mixture was homogenized at 1000 rpm for 5 min using a homogenizer. The mixture was filtered using a filter paper of 0.22 µm. The nanochitosan was collected as the residue [19].

Preparation of silver nanoparticle (AgNPs)

Silver nanoparticles were prepared using the chemical reduction method described by Rashid *et al.* [20], with some modifications. A 40.77 mg of sodium borohydride and 18.16 mg of silver nitrate were weighed and dissolved in 200 mL of ice-cold water at 5 ^{0}C in a separate beaker. Equal volumes of sodium borohydride solution and silver nitrate solution (25 mL) were mixed as follows: the sodium borohydride solution was placed in a volumetric flask with a magnetic stirrer, which was then placed on a heater. The silver nitrate solution was poured into a burette and allowed to drip out, titrating the sodium borohydride solution to a golden-brown color. To determine the presence of silver nanoparticles, 9 mL of the binary mixture was diluted with 1 mL of distilled water and subjected to UV scanning.

Impregnation of CSNPs with AgNPs

CSNPs (0.1 g) was dissolved in a beaker containing 0.1 g of AgNPs, and the mixture was homogenized by placing it on a magnetic stirrer with an electric heater for 5 minutes. After heating, the mixture was filtered, and the residue containing silver nanochitosan was left to dry.

Characterization of the CSNPs/AgNPs

The particles were characterized using a variety of techniques. To examine the morphological structural changes of samples, the scanning electron microscopy (SEM) model (Phenom ProX, by phenom World Einhoven-the Netherlands) was used. Functional group analysis of the materials was conducted using a Buck Scientific M530 USA FTIR. The crystallographic data was obtained using XRD (Bruker D8-Advance multi-purpose) under Cu Kα radiation (λ = 1.5418) and the reflection-transmission spinner stage with Theta-Theta settings. The machine was operated at a tension of 45 VA and current of 40mA. The Gonio Scan was used in conjunction with a Programmable Divergent Slit and a 5mm Width Mask [21]. Differential Scanning Calorimetry (DSC) measurements were taken using a Mettler Toledo STARe SW 11.0 at a heating rate of 10 ^{o}C min^{-1}, with samples heated between 30 °C and 160 °C.

RESULTS AND DISCUSSION

Fig. 1 depicts SEM images of nanochitosan (ArCSNPs) derived from low molecular weight chitosan, nanochitosan (ScCSNPs) derived from snail shell, and their respective silver nanochitosan composites (AgNPs-ArCSNPS and AgNPs-ScCSNPs). The image shows that nanochitosan (Fig. 1a) has a high level of agglomeration, porous surfaces with somewhat quasi-spherical morphologies and a porous surface. On the other hand, silver nanochitosan composite (Fig. 1b) showed lesser agglomeration, more aggregated particles, smooth patches, more porous surface structures with some smooth patches and porous surface structures, indicating that the silver nanoparticles (AgNPs) were aggregated and well distributed into the polymeric matrix. However, the ArCSNPs (Fig. 1c) had a crack rough surface with some porosity, whereas Fig. 1d shows a rough membranous phase deposition on the crack rough surface. The presence of AgNPs may have caused the deposition. The reduction and stabilization process by nanochitosan polymeric chains may be responsible for the formation of porous structures. The porous nature of the material is critical as it enhances surface reactions and would greatly improve antibacterial and biomedical applications [22, 23]. In the work of Britto-Hurtado *et al.* [24],

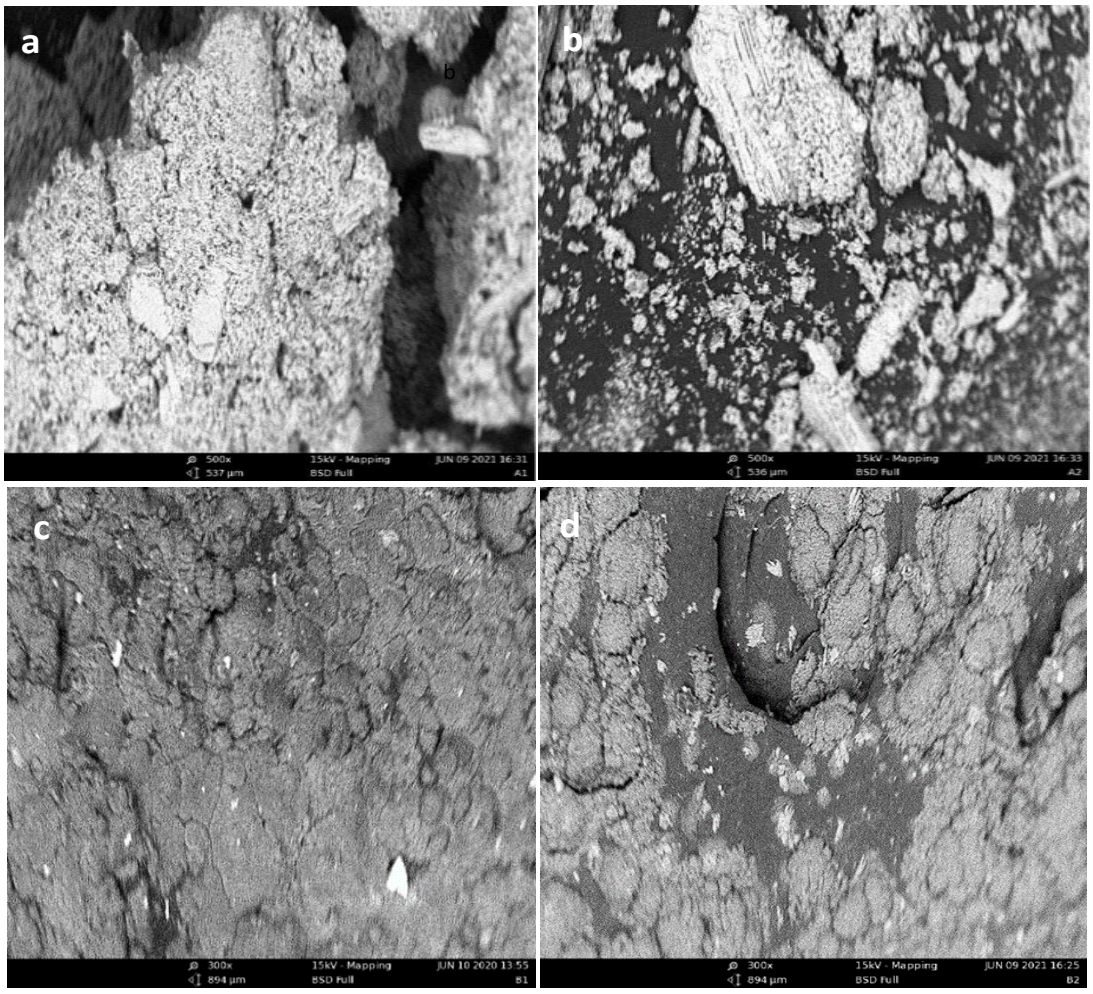

Fig.1 . SEM Images of synthesized (a) ScCSNPs (b) ScCSNPs-AgNPs (c) ArCSNPS (d) ArCSNPS-AgNPs

it was observed that the agglomeration of Au-Pt bimetallic nanoparticles greatly improved their antibacterial activities.

Figs. 2(a-d) illustrate the FTIR spectra of ScCSNPs, ScCSNPs-AgNPs, ArCSNPS, and ArCSNPS-AgNPs, respectively, while Table 1 shows the functional groups associated with corresponding peak wavelength. Fig. 2 shows that nanochitosan (ScCSNPs and ArCSNPS) and its AgNPs nanochitosan composite (ScCSNPs-AgNPs and ArCSNPS-AgNPs) share many peaks of chitosan related to the functional group of hydroxyl (OH) stretching vibration, alkane C–H stretching vibration, and N-H stretching vibration [10]. The peaks 2879 cm^{-1} and 3808 cm^{-1}, 3826.2 and 3415.6 cm^{-1}, 3813.072 and 3695.49 cm^{-1}, 3826.2654 and 3685.015 cm^{-1} are assigned to O-H stretching vibration. The shift in the OH peaks as shown in Table 1 may be due to the presence of silver nanoparticles. Figs. 2(a-d) demonstrate that the various sources of nanochitosan and corresponding AgNPs composites had distinct bands between 3354.1 and 3695.494 cm^{-1}, which indicate N-H stretching. The band at 2167 and 2026 cm^{-1}, as revealed in Figs. 2(a) and 2(b), respectively, may correspond to the alkanyl C=C stretch. In Figs. 2c and 2d, the C=C stretching and bending vibrations are assigned to absorption band at 1610.344 and 904.4cm^{-1}, respectively. The 1992 and 1883.5 cm^{-1} bands can be assigned to C-H stretching from alkane (Figs. 2a and 2b) which are major absorption bands in chitosan. The absorbance values between 1866.1cm^{-1} and 1116.1cm^{-1} are attributed to amine and methyl compounds, CH_3 and C=N stretch, and C-O bond stretch. The peaks around 1420.5cm^{-1} and 756.4 cm^{-1} may have been caused by C-H bond bending probably from aromatic and vinyl compounds, respectively (Figs. 2c and 2d).

Table 1: Functional groups associated with corresponding peak wavelengths

Functional group	ScCSNPs (cm^{-1})	ScCSNPs-AgNPs (cm^{-1})	ArCSNPS (cm^{-1})	ArCSNPS-AgNPs (cm^{-1})
O-H stretch from alcohol	3808.5	3826.2	3813.1	3826.3
N-H stretch	3354.1	3685	3565.9	3415.7
O-H stretch from carboxylic acid	2879.2	3415.6	3695.5	3685.0
C-H stretch	2751.9	3130.5		
O-H stretch from alcohol	2594	1994.1	3396.427	3291.8
C=N Stretch	2534	1874.9		
C=O stretch	2450	2452.4		
C=C stretch	2167	2026		
C-H stretch from alkane	1992	1883.5		
C-H from aldehyde, CH_2 from methylene			2936.4	2812.2
N-H stretch	1613	1621.8	3565.9	3415.7
NH2 glucosamine	1323	1143.5		
C-N stretching	818	1294		
N-CH_3 stretch, S-H from thiols			2785.9	2452.5
C≡C from alkyne, C-H aromatic bending			2205.1	1883.6
N=C=S from thiocyanate, C=C stretch			2033.2	1621.8
CH_3 from methyl			1866.1	1434.8
C=C stretch, C=N stretch			1610.3	1294.0
C-H bend			1420.5	
C-O stretch			1116.1	
C=C bend			904.4	
C-H aromatic bend			756.4	

Murugan *et al.* [25] observed a similar peak at 789 cm^{-1} which was believed to correspond to aromatic C–H bending in bio-encapsulated chitosan-Ag nanocomplex. A significant absorption band of nanochitosan was also observed at 1323 cm^{-1} (Fig. 2a), which correspond to the free -NH_2 group in the glucose amine. C-N has a peak at 818 cm^{-1}, which agrees well with similar studies conducted by other scholars [26, 27]. A vibrational mode of the amide (NH) C=O stretching was observed at 1613 cm^{-1}. In comparison to chitosan, the spectra of Ag chitosan nanoparticles composites showed a few alternations. The FTIR spectra of silver nanochitosan (ScCSNPs-AgNPs and ArCSNPs-AgNPs) show a decreasing and shifting of peak to 3415.1 and 3685 cm^{-1}, which are attributed to vibrational stretching of the N-H and O-H groups. This is because hydrogen bonding is enhanced in ScCSNPs-AgNPs and ArCSNPs-AgNPs, implying Ag chelation with both amino and hydroxyl groups of chitosan [27, 28]. The introduction of AgNPs to CSNPs may have resulted in a shift in the peak of the -NH_2 group and C-N at 1434.7 and 1294 cm^{-1}, respectively (Fig. 2b). The shift of band from 1613 to 1621.8 cm^{-1} is attributed to the binding of (NH) C=O group with Ag nanoparticles. In general, the stretching and bending frequency peaks could be attributed to the stretching of chitosan's carbon and hydrogen bonds. The peaks could also indicate that a carbonyl group formed amino acid residues that capped AgNP, implying that molecules capping chitosan-Ag nanoparticles contained both free and bound amide groups [25, 29].

Fig. 3 depicts the X-ray diffraction analysis results of nanochitosan and its respective silver nanoparticles composite. The results demonstrate the crystallinity of the nanochitosan and its silver nanochitosan obtained from snail shells and commercially purchased chitosan. The peaks of nanochitosan were observed at $2\theta = 8.1^{o}$ (ScCSNPs) and 20.1^{o} (ArCSNPs), which are closer to the characteristic peak of $2\theta = 9.1^{o}$ and 19.9^{o} mentioned

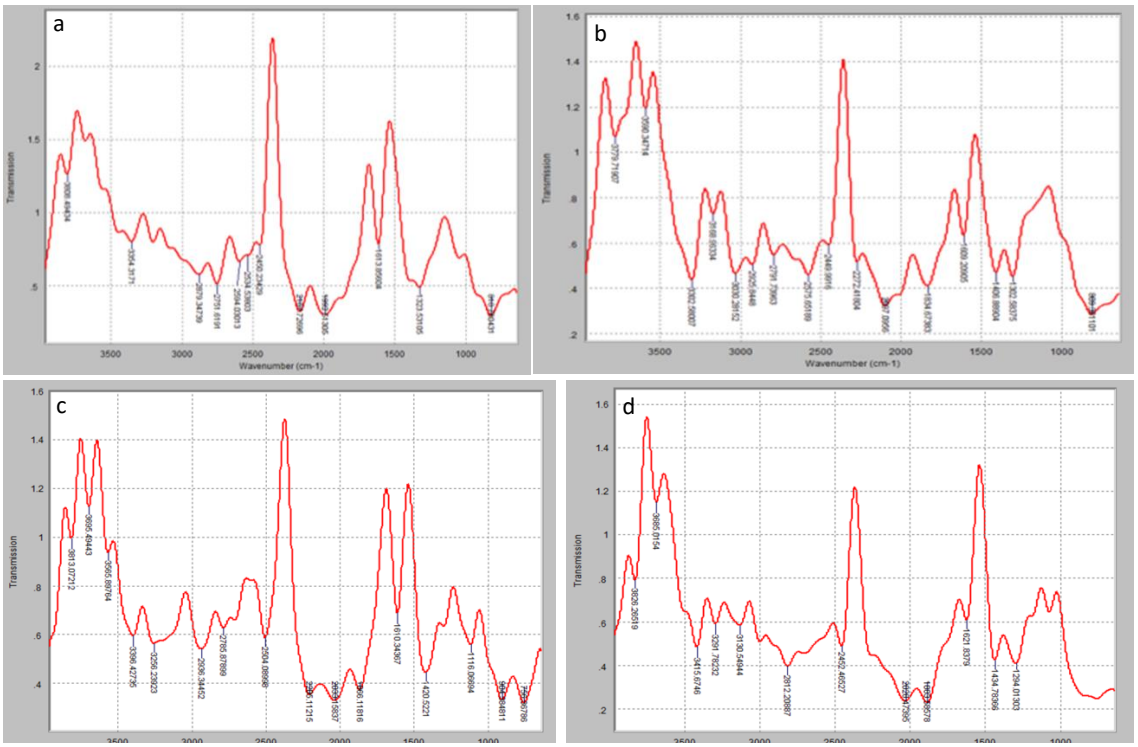

Fig. 2. FTIR spectrum of (a) ScCSNPs (b) ScCSNPs.AgNPs (c) ArCSNPs (d) ArCSNPs-AgNPs

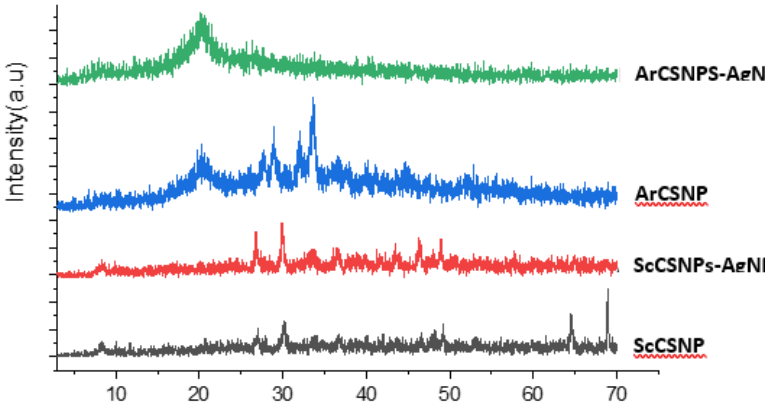

Fig. 3. X-Rays diffraction patterns of nanochitosan (ScCSNPs and ArCSNPS) and its respective silver nanoparticles composite (ScCSNPs-AgNPs and ArCSNPS-AgNPs)

by Dara *et al.* [30]. The same peak was observed in their AgNPs nanochitosan composite. As also observed by Zahedi *et al.* [31] and Dara *et al.* [30], the peak at 2θ = 20.1° indicates the high degree of chitosan and their crystal lattice constant α corresponding to 4.4. As shown in Fig. 3, the peaks at 2θ = 33.6°, 43.33°, and 46.5° appear on the spectra of ScCSNPs-AgNPs which do not appear on the spectra of ScCSNPs but are devoid of peaks at 64.7° and 69.1°. Further, the sharp peaks at 2θ = 27.6, 28.9, 32, and 33.9° on ArCSNPs pattern are absent on ArCSNPs-AgNPs. The presence of AgNPs in the polymeric matrix of the nanochitosan may explain the appearance and disappearance of these peaks. The Bragg reflection's numbers with 2θ values of 43.33° and 64.7° referring to (200) and (220),

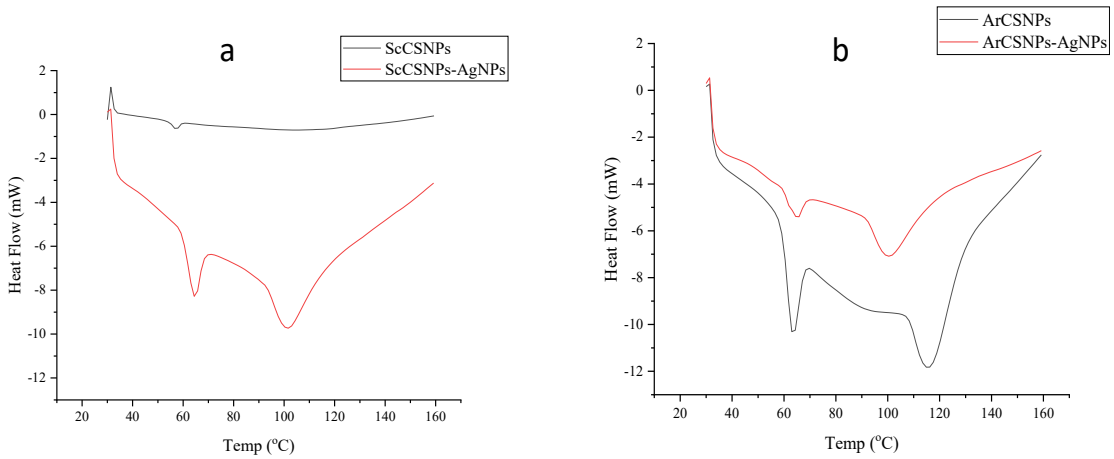

Fig. 4. Differential Scanning Calorimetry thermogram of (a) ScCSNPs and ScCSNPs-AgNPs (b) ArCSNPS and ArCSNPS-AgNPs

respectively, indicate the spherical and crystalline nature of Ag NPs [1, 32]. The sharp diffraction peaks represent a large particle, whereas the broad diffraction peaks represent a smaller particle. The XRD pattern of AgNPs nanochitosan reveals the polymeric nanoparticles' crystalline nature.

Fig. 4 shows the DSC thermograms of nanochitosan (ScCSNPs and ArCSNPS) and its respective silver nanoparticles composite (ScCSNPs-AgNPs and ArCSNPS-AgNPs) at a heating rate of 10 °C/min with various compositions. Except for ScCSNPs (Fig. 4a), which showed heat release (exothermic) as a result of crystallization, all samples showed a glass transition (Tg) temperature, indicating good miscibility between nanochitosan matrix at the start of the heat flow. This resulted in a crystal melting temperature of 60 °C. The appearance of Tg in Fig. 4a for ScCSNPs-AgNPs, as well as the difference in Tg size in Fig. 4b, may be due to the incorporation of AgNPs into the nanochitosan matrix, which can be attributed to the higher mobility of the polymer macromolecules [33, 34].

CONCLUSIONS

SEM, FTIR, DSC and XRD were used to affirm the synthesis of nanochitosan and its silver nanochitosan. The SEM and XRD results revealed the porous, agglomeration, and crystalline structure of the ScCSNPs, ScCSNPs-AgNPs, ArCSNPs and ArCSNPs-AgNPs. The crystal structure and the presence of AgNPs were also confirmed by DSC analysis. The presence of hydroxyl, amino, and alkyl groups in nanochitosan and its silver nanochitosan counterpart was revealed by FTIR analysis. Even with the presence of AgNPs, the amino group can also serve as available charged sites for interaction with negatively charged bacterial cells, making them suitable for adsorption and antimicrobial application. Chitosan extracted from biowaste (snail shell) can be an effective tool for controlling microbial pathogens, thereby addressing two major public health issues: waste recycling and vector control. This study indicated that chitosan extract from snail shell and its silver nanochitosan composite could potentially substitute commercially low molecular chitosan and its silver nanochitosan composite, respectively, in all the various applications of chitosan and its derivatives. However, the use of natural product extracts as agents of deproteination, demineralization, and deacetylation during the extraction of chitosan from biowastes before modification and impregnation with silver nanoparticle is highly recommended.

ACKNOWLEDGEMENTS

The authors would like to thank Isa Yakubu of the Department of Chemical Engineering, Ahmadu Bello University, Zaria and Isaac I. Okorie of Centre for Genetic Engineering and Biotechnology (Step-B), Federal University of Technology, Minna for their technical assistance.

FUNDING

The authors did not receive support from any organization for the submitted work.

CONFLICT OF INTEREST

The authors declare no conflicts of interest.

AUTHOR CONTRIBUTIONS

The study conception and design were performed by Vincent Nwalieji Okafor. Material preparation, data collection and analysis were performed by Vincent Nwalieji Okafor, Akinyele Abimbola Bankole, Iwe Assumpta Daberechukwu, and Mbume Oluchukwu Francisca. The first draft of the manuscript was written by Akinyele Abimbola Bankole and all authors commented on previous versions of the manuscript. All authors read and approved the final manuscript.

DATA AVAILABILITY

The datasets generated during and/or analyzed during the current study are available from the corresponding author on reasonable request.

REFERENCES

1. Alshehri MA, Aziz AT, Trivedi S, Panneerselvam C. Efficacy of chitosan silver nanoparticles from shrimp-shell wastes against major mosquito vectors of public health importance. 2020;9(1):675-84. doi:10.1515/gps-2020-0062
2. Yanat M, Schroën K. Preparation methods and applications of chitosan nanoparticles; with an outlook toward reinforcement of biodegradable packaging. Reactive and Functional Polymers. 2021;161:104849. https://doi.org/10.1016/j.reactfunctpolym.2021.104849
3. Al-Zahrani SS, Bora RS, Al-Garni SM. Antimicrobial activity of chitosan nanoparticles. Biotechnology & Biotechnological Equipment. 2021;35(1):1874-80. 10.1080/13102818.2022.2027816
4. Trung TS, Tram LH, Van Tan N, Van Hoa N, Minh NC, Loc PT, et al. Improved method for production of chitin and chitosan from shrimp shells. Carbohydrate Research. 2020;489:107913. https://doi.org/10.1016/j.carres.2020.107913
5. Klongthong W, Muangsin V, Gowanit C, Muangsin N. Chitosan Biomedical Applications for the Treatment of Viral Disease: A Data Mining Model Using Bibliometric Predictive Intelligence. Journal of Chemistry. 2020;2020:6612034. 10.1155/2020/6612034
6. Aranaz I, Mengibar M, Harris R, Panos I, Miralles B, Acosta N, et al. Functional Characterization of Chitin and Chitosan. Current Chemical Biology. 2009;3(2):203-30. 10.2174/187231309788166415
7. Islam S, Bhuiyan MAR, Islam MN. Chitin and Chitosan: Structure, Properties and Applications in Biomedical Engineering. Journal of Polymers and the Environment. 2017;25(3):854-66. 10.1007/s10924-016-0865-5
8. Dash S, Kumar M, Pareek N. Enhanced antibacterial potential of berberine via synergism with chitosan nanoparticles. Materials Today: Proceedings. 2020;31:640-5. https://doi.org/10.1016/j.matpr.2020.05.506
9. Gadkari RR, Suwalka S, Yogi MR, Ali W, Das A, Alagirusamy R. Green synthesis of chitosan-cinnamaldehyde cross-linked nanoparticles: Characterization and antibacterial activity. Carbohydrate Polymers. 2019;226:115298. https://doi.org/10.1016/j.carbpol.2019.115298
10. Romainor ANB, Chin SF, Pang SC, Bilung LM. Preparation and characterization of chitosan nanoparticles-doped cellulose films with antimicrobial property. Journal of Nanomaterials. 2014;2014.
11. Abdallah Y, Liu M, Ogunyemi SO, Ahmed T, Fouad H, Abdelazez A, et al. Bioinspired Green Synthesis of Chitosan and Zinc Oxide Nanoparticles with Strong Antibacterial Activity against Rice Pathogen Xanthomonas oryzae pv. oryzae. Molecules [Internet]. 2020; 25(20). 10.3390/molecules25204795
12. Okafor V, Umenne C, Tabugbo B, Okonkwo C, Obiefuna J, Okafor U, et al. Potentiality of Diethylamine as Agent of Deproteination and Deacetylation in the Extraction of Chitosan from Scylla serrata Shell. Chemistry and Materials Research. 2020;Vol. 12:35-45. 10.7176/CMR/12-7-07
13. Teli MD, Sheikh J. Extraction of chitosan from shrimp shells waste and application in antibacterial finishing of bamboo rayon. International Journal of Biological Macromolecules. 2012;50(5):1195-200. https://doi.org/10.1016/j.ijbiomac.2012.04.003
14. Pakizeh M, Moradi A, Ghassemi T. Chemical extraction and modification of chitin and chitosan from shrimp shells. European Polymer Journal. 2021;159:110709. https://doi.org/10.1016/j.eurpolymj.2021.110709
15. Agoha EEC, editor Biomaterials from Periwinkle Shells: Composition and Functional Properties. World Congress on Medical Physics and Biomedical Engineering 2006; 2007 2007//; Berlin, Heidelberg: Springer Berlin Heidelberg.
16. Isa M. Extraction and Characterization of Chitin and Chitosan from Mussel Shell. Civil and Environmental Research. 2013;3:108-14.
17. Okoya A, Akinyele A, Amuda O, Ofoezie E. Chitosan Grafted Modified Maize Cob for Removal of Lead And Chromium from Wastewater. Ethiopian Journal of Environmental Studies and Management. 2016;8:881. 10.4314/ejesm.v8i2.3S
18. Wijayadi LJ, Rusli TR. Characterized and synthesis of chitosan nanoparticle as nanocarrier system technology. IOP Conference Series: Materials Science and Engineering. 2019;508(1):012143. 10.1088/1757-899X/508/1/012143
19. Rashid MU, Bhuiyan MKH, Quayum ME. Synthesis of Silver Nano Particles (Ag-NPs) and their uses for Quantitative Analysis of Vitamin C Tablets. Dhaka University Journal of Pharmaceutical Sciences. 2013;12(1):29-33. 10.3329/dujps.v12i1.16297
20. Abdallah Y, Ogunyemi SO, Abdelazez A, Zhang M, Hong X, Ibrahim E, et al. The Green Synthesis of MgO Nano-Flowers Using Rosmarinus officinalis L. (Rosemary) and the Antibacterial Activities against Xanthomonas oryzae pv. oryzae. BioMed Research International. 2019;2019:5620989. 10.1155/2019/5620989
21. Jeyaraman DM, R.Vignesh, N.Sumathi. EXTRACTION, CHARACTERIZATION AND APPLICATIONS OF CHITOSAN FROM FISH SCALES. 2017. 10.21884/IJMTER.2017.4131.Q8NJR
22. Udenni Gunathilake TMS, Ching YC, Ching KY, Chuah CH, Abdullah LC. Biomedical and Microbiological Applications of Bio-Based Porous Materials: A Review. Polymers [Internet]. 2017; 9(5). 10.3390/polym9050160
23. Yahya EB, Jummaat F, Amirul AA, Adnan AS, Olaiya

NG, Abdullah CK, et al. A Review on Revolutionary Natural Biopolymer-Based Aerogels for Antibacterial Delivery. Antibiotics [Internet]. 2020; 9(10). 10.3390/antibiotics9100648

24. Britto Hurtado R, Cortez-Valadez M, Flores-Lopez NS, Flores-Acosta M. Agglomerates of Au-Pt bimetallic nanoparticles: synthesis and antibacterial activity. Gold Bulletin. 2020;53(2):93-100. 10.1007/s13404-020-00277-y
25. Murugan K, Jaganathan A, Suresh U, Rajaganesh R, Jayasanthini S, Higuchi A, et al. Towards Bio-Encapsulation of Chitosan-Silver Nanocomplex? Impact on Malaria Mosquito Vectors, Human Breast Adenocarcinoma Cells (MCF-7) and Behavioral Traits of Non-target Fishes. Journal of Cluster Science. 2017;28(1):529-50. 10.1007/s10876-016-1129-1
26. Kannan RRR, Arumugam R, Ramya D, Manivannan K, Anantharaman P. Green synthesis of silver nanoparticles using marine macroalga Chaetomorpha linum. Applied Nanoscience. 2013;3(3):229-33. 10.1007/s13204-012-0125-5
27. Murugan K, Anitha J, Suresh U, Rajaganesh R, Panneerselvam C, Aziz AT, et al. Chitosan-fabricated Ag nanoparticles and larvivorous fishes: a novel route to control the coastal malaria vector Anopheles sundaicus? Hydrobiologia. 2017;797(1):335-50. 10.1007/s10750-017-3196-1
28. Chen Q, Jiang H, Ye H, Li J, Huang J. Preparation, Antibacterial, and Antioxidant Activities of Silver/Chitosan Composites. Journal of Carbohydrate Chemistry. 2014;33(6):298-312. 10.1080/07328303.2014.931962
29. Sathyavathi R, Krishna MB, Rao SV, Saritha R, Rao DN. Biosynthesis of Silver Nanoparticles Using Coriandrum Sativum Leaf Extract and Their Application in Nonlinear Optics. Advanced Science Letters. 2010;3(2):138-43. 10.1166/asl.2010.1099
30. Dara PK, Mahadevan R, Digita PA, Visnuvinayagam S, Kumar LRG, Mathew S, et al. Synthesis and biochemical characterization of silver nanoparticles grafted chitosan (Chi-Ag-NPs): in vitro studies on antioxidant and antibacterial applications. SN Applied Sciences. 2020;2(4):665. 10.1007/s42452-020-2261-y
31. Zahedi S, Safaei Ghomi J, Shahbazi-Alavi H. Preparation of chitosan nanoparticles from shrimp shells and investigation of its catalytic effect in diastereoselective synthesis of dihydropyrroles. Ultrasonics Sonochemistry. 2018;40:260-4. https://doi.org/10.1016/j.ultsonch.2017.07.023
32. Kalaivani R, Maruthupandy M, Muneeswaran T, Hameedha Beevi A, Anand M, Ramakritinan CM, et al. Synthesis of chitosan mediated silver nanoparticles (Ag NPs) for potential antimicrobial applications. Frontiers in Laboratory Medicine. 2018;2(1):30-5. https://doi.org/10.1016/j.flm.2018.04.002
33. Sonseca A, Madani S, Rodríguez G, Hevilla V, Echeverría C, Fernández-García M, et al. Multifunctional PLA Blends Containing Chitosan Mediated Silver Nanoparticles: Thermal, Mechanical, Antibacterial, and Degradation Properties. Nanomaterials [Internet]. 2020; 10(1). 10.3390/nano10010022
34. Liu X, Wang T, Chow LC, Yang M, Mitchell JW. Effects of Inorganic Fillers on the Thermal and Mechanical Properties of Poly(lactic acid). International Journal of Polymer Science. 2014;2014:827028. 10.1155/2014/827028